

# LARGE SCALE EXPERIMENTS DATA ANALYSIS FOR ESTIMATION OF HYDRODYNAMIC FORCE COEFFICIENTS

## PART 2: FREQUENCY DOMAIN ANALYSIS

*Morteza Naghipour*

*Department of Civil Engineering, Mazandaran University  
Babol, Iran, m-naghi@tech.umz.ac.ir*

**(Received: November 6, 2001 – Accepted in Revised Form: December 22, 2002)**

**Abstract** This paper describes the various frequency domain methods which may be used to analyze experiments data on the force experienced by a circular cylinder in wave and current to estimate drag and inertia coefficients for use in Morison's equation. An additional approach, system identification techniques (SIT) is also introduced. A set of data obtained from experiments on heavily roughened circular cylinders in waves and simulated current has been analyzed by all these techniques. The resulting force coefficients are then used to predict the force from separate experiments-results, which have not used in the analysis. The root mean square error and bias in the estimation of maximum force in each wave cycle is used as a measure of predictive accuracy and as a basis for comparing the analysis techniques. The case when wave particle kinematics must be inferred from water surface elevation is also considered. It is found that when water particle kinematics are not possible to be measured directly and have to be inferred from surface elevation then using a system identification approach, the predictive errors increase considerably.

**Key Words** Morison's Equation, System Identification Techniques, Stokes Theory, Wave Reflection, Particle Kinematics

**چکیده** این مقاله روشهای مختلف در حوزه فرکانسی مورد استفاده در آنالیز داده‌ها به منظور تخمین ضرایب هیدرودینامیکی درگ و اینرسی در معادله موریسون روی استوانه‌های واقع در امواج و جریانات پایا را تشریح نموده و روش SIT را معرفی می‌کند. داده‌های بدست آمده از آزمایش بر سیلندرهای استوانه‌ای با سطح کاملاً زبر واقع در امواج و جریانات شبیه‌سازی شده توسط این روشها آنالیز گردیده‌اند. سپس ضرایب بدست آمده از این آنالیز بر یک سری داده‌های دیگر بکار گرفته شده‌اند. برای مقایسه روشهای مختلف آنالیز در هر سیکل موج از جذر میانگین مربعات RMSE و میانگین خطای نرمال MNE استفاده شده است. همچنین حالتی که در آن سینماتیک ذرات آب می‌بایست از سطح دریا بدست آید، مورد بررسی قرار گرفته است. ملاحظه گردید که وقتی که سینماتیک ذرات آب جهت اندازه‌گیری مستقیماً ممکن نباشد و باید از سطح دریا با استفاده از تئوری موج تعیین گردد، استفاده از روش SIT خطای نیروهای تخمینی بطور قابل ملاحظه ای کاهش می‌دهد.

### 1. INTRODUCTION

There has been a considerable volume of experimental research undertaken to estimate the force coefficients in Morison's equation, which parallels the growth in the number of tubular jacket structures used for offshore oil and gas recovery. Much of the early work was undertaken at small-scale and the results

from these small-scale experiments are not directly applicable.

The 3-dimensional random waves found offshore can be reproduced in multi-directional wave basins in the laboratory but this is usually on too small scale to achieve post-critical flow conditions for large a wide range of KC for circular cylinders unless the relative roughness coefficient ( $k =$

average roughness height / cylinder diameter) is very large. To achieve the required Re experiments have been undertaken in various flow conditions using various techniques including:

- steady flow obtained using a cylinder suspended beneath a carriage in a towing tank, oscillating water in a large U-tube past a fixed cylinder (e.g. [1])
- moving cylinders using a bi-directional carriage [2]
- regular and random long-crested waves in a 2-dimensional wave flume (e.g. [3]).

The last provides the most realistic representation of offshore conditions currently available in the laboratory and the experiments described and discussed in this paper were undertaken in a large 2-D wave flume.

Experiments have been undertaken offshore in real sea waves, notably at the Christchurch Bay Tower (CBT) off the south coast of England [4] and at the Ocean Test Structure (OTS) in the Gulf of Mexico. Unfortunately measurements offshore at the time of these experiments were difficult and accurate simultaneous measurements of wave particle kinematics, wave surface elevation and wave force close to the axis of a test cylinder with a well-defined surface roughness have not all been obtained. However these experiments have provided some very useful data obtained in the most realistic possible conditions.

A variety of procedures have been used to analyze experiment data in the context of Morison's equation and to predict Cd and Cm. The methods used in frequency domain analysis are described in Section 3 of this paper.

To reflect the usual offshore design and assessment procedure the above test can be altered by ignoring the measured particle kinematics and just using the surface elevation from the second part of the experimental data. The particle kinematics is then predicted using a wave theory to provide the input into the predicted Morison force time series. In this case it is appropriate in the analysis stage to estimate the particle kinematics from the surface elevation (using the same wave theory) and to use these estimates to obtain corresponding force coefficients.

On this basis it has been possible to compare

both the various analysis procedures, and the ability of the various wave theories to predict particle kinematics for this particular set of experiments. It is also possible to give some measure of the uncertainty and bias involved in using Morison's equation for the prediction of in-line forces which should be helpful in structural reliability calculations and structural assessments.

The next section of the paper describes the experiments that were undertaken as part of an EC/MTD funded project in the Delft Hydraulics Laboratories (DHL) long wave flume at DeVoorst in Holland. The third section describes the various methods for the prediction of force coefficients from experiment data. The fourth section deals with the prediction of wave particle kinematics from different wave theories. The fifth section presents a discussion of the results from the analysis of the experiment data using the various approaches and the associated mean errors and bases. Finally some conclusions are drawn.

## 2. DESCRIPTION OF THE EXPERIMENTS

A series of experiments were done to examine the wave loading on two large-scale circular cylinders in the Delft Hydraulic Laboratory's (DHL) Delta wave flume on the northeast Polder near Emmeloord in Holland. The flume is 230m long, 5m wide, 7m deep and during all tests was filled with water to a depth of about 5m. The waves were generated either in regular or random form by a programmable piston-type wave maker. Most of their energy was dissipated at the other end of the flume through the use of a compound concrete beach and a little part of energy was reflected so that the maximum reflection coefficient was about 10%. The beach consists of three different slopes, 1:4, 1:6 and 1:16 with horizontal lengths, 12m, 18m and 16m respectively.

Regular random waves were generated with the range of periods from about 3 to 10 seconds. The wave heights were up to about 2m over most of the range of periods and at some frequencies breaking waves occurred occasionally. The results presented in this paper are for experiments in long crested random waves with a significant wave height of

1.5 m and a peak period of 5.9 second.

For simulating the effects of current and combined wave/current flows the flume was equipped with a towing carriage system with dimensions of about 8m by 6m in plan. It runs on a set of rails fixed on the top of the flume walls and can attain steady velocities up to 1m/s. For the experiments analyzed here the carriage speed was 1m/s and 0.5m/s and the towing distance was approximately 110m. The two vertical cylinders used for the experiments described in this paper had diameters of 0.21m (small) and 0.5m (large) and were mounted in turn on the towing carriage and at a fixed location (16m from the toe of the beach and 164m from wave maker) in the flume. A mobile cylinder in the flume mounted on the carriage is given in [5, 6]. Both cylinders were manufactured from stainless steel and were covered with the roughness pattern. The roughness elements were cast in fiberglass in the form of two semi-circular shells which were strapped to the cylinder giving an effective roughness ratio  $k_r / D$  (where  $k_r$  is average height of roughness projections and  $D$  is cylinder diameter) was 0.038 and a corresponding effective diameter of the large and small rough cylinders of 0.513m and 0.216m respectively.

In the mobile cases the cylinder was rigidly fixed to the carriage at the top and had a heavy horizontal plate rigidly attached at the bottom. The instruments important to the author's work are the force sleeves, wave height gauges, the water particle velocity meters and static pressure probes.

Measurements of the wave force time series for both cylinders were obtained using two-component strain-gauged transducers, each 0.5D long and capable of measuring both the in-line (in the direction of wave propagation) and transverse forces (orthogonal to the in-line force).

The small cylinder had 5 force sleeves of which four were below the mean water level (MWL), and the large cylinder had two force measuring sleeves below the MWL. The upper two force sleeves on the small cylinder were close to the free surface and, dependant upon the wave conditions used, were not continuously immersed in the waves. The author has examined the data

from all the force sleeves but the results presented in this paper were derived from force measurements at position 2 as shown in [5] for both the small and the large cylinder. This decision was made so that any water free surface effects and bottom effects on the results presented were negligible.

Water surface elevation was measured using two wave gauges, resistance wave gauge and follow wave gauge. Water particle velocities were always measured at the elevation of the force sleeves by means of two different kinds of instrumentation i.e. electromagnetic flow meters (EMF) and perforated ball velocity meters (PVM).

The A/D converter digitized the analogue voltages from the wave probes and load cell. A sampling frequency of 40 Hz was used in the experiments for all the data has been stored in binary format as 2 byte integers.

### 3. METHOD FOR ESTIMATING FORCE COEFFICIENTS

#### 3.1 Estimating of Force Coefficients from the Kinematics and Measurement Force Using System Identification Techniques (SIT)

The basic object of system identification for an input/output physical system is to obtain a functional which maps the input or excitation to the output or response. The different techniques of this method are widely used in parameter estimation of non-linear systems [7].

Kaplan et al. [8] used a method of system identification for determining the Morison's equation coefficient values. A slightly different method based on a block structural system that has been developed in [9] was used in [10, 11] for non-linear frequency modeling of random wave force on a pile.

Assuming that  $u$  is normally distributed with mean zero and standard division  $\sigma$ , Borgman [12] determined the best linear, cubic and quintic approximation for  $u|u|$  term in the least square sense. He showed that the linear approximation offers a reasonable solution only to about two standard deviations whilst the cubic is good to

more than three and the quintic to about four standard deviations. The quintic approximation is thus only slightly better than the cubic, which is quite an improvement over the linear expression. Considering the least square approximation to  $|u|$  by a third-order polynomial [9] the resulting linearization in the Morison's equation for velocity is given as:

$$|u| = \sigma_u^2 \left[ \sqrt{\frac{8}{\pi}} \left( \frac{u}{\sigma_u} \right) \right] \quad (\text{Linear})$$

$$|u| = \sigma_u^2 \left\{ \sqrt{\frac{2}{\pi}} + \left[ \frac{1}{3} \left( \frac{u}{\sigma_u} \right)^3 \right] \right\} \quad (\text{Cubic})$$

$$|u| = \sigma_u^2 \left\{ \sqrt{\frac{2}{\pi}} \left[ \frac{3}{4} \left( \frac{u}{\sigma_u} \right) + \frac{1}{2} \left( \frac{u}{\sigma_u} \right)^3 - \frac{1}{60} \left( \frac{u}{\sigma_u} \right)^5 \right] \right\} \quad (\text{Quintic}) \quad (1)$$

where  $\sigma_u$  is standard deviation of  $u$ . In a co-existing wave and current field  $u$  has a non-zero mean normal distribution ( $\mu_u = U$  where  $U$  is the current speed) and the least-square linear estimate for  $|u|$  is determined [12] by minimizing:

$$E = \int_{-\infty}^{\infty} (|u| - b_0 - b_1 u) \frac{1}{\sigma_u \sqrt{2\pi}} \exp\left[-\frac{(u - U)^2}{2\sigma_u^2}\right] du \quad (2)$$

where  $b_0$  and  $b_1$  are given by:-

$$b_0 = \sigma_u^2 [(1 - \gamma^2)(2Z(\gamma) - 1) + 2\gamma z(\gamma)] \quad (3)$$

$$b_1 = 2\sigma_u [\gamma(2Z(\gamma) - 1) + 2z(\gamma)]$$

where  $\gamma = \mu_u / \sigma_u$  is a parameter measuring the strength of the current,  $\mu_u$  is mean value of water particle velocity which is equal with current speed and

$$z(\gamma) = (2\pi)^{-0.5} \exp(-0.5\gamma^2)$$

$$Z(\gamma) = \int_0^\gamma z(x) dx \quad (4)$$

In a linear wave force model using the linear approximation (Equations 1), the Morison's equation

(with no current) can be written as:

$$f(t) = C\dot{u}(t) + Ku(t) \quad (5)$$

where

$$K = \rho DC_d \sqrt{\frac{2}{\pi}} \sigma_u \quad \text{and} \quad C = \frac{\pi}{4} \rho D^2 C_m \quad (6)$$

where  $D$  is cylinder diameter and  $\rho$  is density of water. For the linear system described by Equation 5 if a constant amplitude harmonic input given by

$$f(t) = f_0 e^{i2\pi ft} \quad (7)$$

is applied, the corresponding output  $u(t)$  will be given by

$$u(t) = T(f) f_0 e^{i2\pi ft} \quad (8)$$

Substituting the Equations 7 and 8 into the Equation 5, then the system frequency response function (FRF) is given

$$T(f) = \frac{1}{K + i2\pi fC} \quad (9)$$

Therefore in the frequency domain

$$U(f) = T(f)F(f) \quad (10)$$

where  $U(f)$  and  $F(f)$  are the Fourier transfer functions of water particle velocity and measured force respectively.

Or

$$F(f) = \frac{1}{T(f)} U(f) = T_{uf}(f) U(f) = (K + i2\pi fC) U(f) \quad (11)$$

where  $T_{uf}(f)$  is the linear transfer function between velocity ( $u$ ) and force ( $f$ ).

Now by choosing two non-dimensional real parameters  $C_{mf}(f)$  and  $C_{df}(f)$ :

$$\text{Re}[T_{uf}(f)] = \rho DC_{df}(f) \sqrt{\frac{2}{\pi}} \sigma_u \quad (12)$$

$$\text{Im}[T_{uf}(f)] = 2\pi f \rho \frac{\pi D^2}{4} C_{mf}(f) \quad (13)$$

and using suitable experiment data from random wave experiments for measured force and corresponding water particle velocity one can estimate (e.g. [13, 14]) the transfer function:

$$T_{uf}(f) = \frac{G_{uf}(f)}{G_{uu}(f)} \quad (14)$$

where  $G_{uu}(f)$  is the one-sided spectral density function of the input i.e. measured particle velocity and  $G_{uf}(f)$  is the cross-spectral density of the input and output i.e. measured particle velocity and measured force. Finally by using Equations 12 and 13 estimates of the hydrodynamic coefficients can be found as functions varying with frequency.

Furthermore as

$$G_{vv}(f) = |T_{uf}(f)|^2 G_{uu}(f) = \frac{|G_{uf}(f)|^2}{G_{uu}(f)} \quad (15)$$

then the ordinary coherence function is

$$\gamma_{uf}^2 = \frac{|G_{uf}(f)|^2}{G_{uu}(f)G_{ff}(f)} \quad (16)$$

and the corresponding noise output spectrum is

$$G_{nn}(f) = [1 - \gamma_{uf}^2(f)]G_{ff}(f) \quad (17)$$

This gives a measure of the correctness of the model in describing the experiment data. Obviously the noise spectrum will be small for a good fit.

This model can be extended for a non-linear form of Morison's equation where the cubic approximation is used in this paper.

In this model,  $\alpha = (\frac{2}{9\pi\sigma^2})^{0.5}$ ,  $T_1$  and  $T_n$

represent the transfer function of the linear and non-linear parts of Morison's equation.

Morison's equation is then written using the cubic approximation as:

$$f(t) = K_M \dot{u}(t) + K_{D1} u(t) + K_{D2} u(t)^3 \quad (18)$$

where

$$\begin{aligned} K_M &= C_m \rho \pi D^2 / 4, \quad K_{D1} = 3\alpha \sigma^2 C_d \rho D / 2 \\ K_{D2} &= \alpha C_d \rho D / 2 \end{aligned} \quad (19)$$

In this case, using the harmonic probing of the Volterra series [15], the second-order frequency response function can be shown to be zero as the nonlinearity is an odd power. The first and third order ones can be determined [16] as:

$$T_1(f) = K_{D1} + i2\pi f K_M \quad \text{and} \quad T_3(f) = K_{D2} / 6 \quad (20)$$

The Fourier transformation of Morison's equation is then given by:

$$F(f) = U(f)(K_{D1} + i2\pi f K_M) + (\frac{K_{D2}}{6})(U^{*3}(f)) \quad (21)$$

where  $U^{*3}(f)$  is a triple convolution of  $U(f)$  with itself.

Decomposing the Morison force into linear and non-linear components yields the frequency response functions of drag and inertial loading ( $T_1$  and  $T_3$ ) which in turn yield the expressions below for  $C_{df}(f)$  and  $C_{mf}(f)$ :

$$\begin{aligned} C_{mf}(f) &= \frac{\text{Im}(T_1)}{2\pi f (\frac{\rho \pi D^2}{4})} \\ C_{df}(f) &= \frac{\text{Re}(T_1)}{3\alpha \sigma^2 (\frac{\rho D}{2})} \end{aligned} \quad (22)$$

The above method may be extended to the case of combined current and waves.

**3.2 Estimating of Force Coefficients from Wave Surface Elevation and Measurement Force Using (SIT)** Using linear wave theory the kinematics can be obtained from surface

elevation as:

$$u = \sum q_i \eta_i, \quad \eta = \sum \frac{H_i}{2} \cos(k_i x - \omega_i t)$$

$$q_i = \frac{2\pi \cosh k_i z}{T_i \sinh k_i d} \quad (23)$$

where  $d$  is the still water depth,  $z$  is the elevation of the measured velocity above the seabed,  $\eta$  is the surface elevation,  $q_i$  is the horizontal velocity transfer function,  $k$  is the wave number which is related to the wave angular frequency  $\omega$  through the linear dispersion relationship:

$$\omega_i = 2\pi f_i = \sqrt{gk_i \tanh k_i d} \quad (24)$$

where  $g$  is the acceleration of gravity and  $f$  is frequency.

If the wave has one frequency component then the kinematics can be predicted without any difficulty from surface elevation as

$$u(t) = \frac{2\pi \cosh kz}{T \sinh kd} \eta(t) = q\eta(t) \quad (25)$$

In this case in wave-by-wave analysis linear theory is assumed. Then using the linear approximation Morison's equation can be written as:

$$f(t) = C\dot{\eta}(t) + K\eta(t) \quad (26)$$

where  $K = \rho DC_d \sqrt{\frac{2}{\pi}} q^2 \sigma_\eta$  and  $C = \frac{\pi}{4} \rho D^2 q C_m$ .

The case when reflection is not negligible, Equation 26 can be corrected with a coefficient  $C_r^*$  [17]. For DHL data analysis it can be considered as a constant, 0.05 [6].

For a linear system if a constant amplitude harmonic input is used then the system frequency response function (FRF) is given by:

$$T(f) = \frac{1}{K + i2\pi f C} \quad (27)$$

$$F(f) = \frac{1}{T(f)} H(f) = T_{\eta f}(f) H(f) = (K + i2\pi f C) H(f) \quad (28)$$

where  $T_{\eta f}(f)$  is the linear transfer function between surface elevation and force and  $H(f)$  and  $F(f)$  are the Fourier transformations of surface elevation and force respectively. Then the two non-dimensional real parameters  $C_{mf}(f)$  and  $C_{df}(f)$  can be found from the following equations:

$$\text{Re}[T_{\eta f}(f)] = \rho DC_{df}(f) \frac{g}{d} \sqrt{\frac{2}{\pi}} \sigma_\eta$$

$$\text{Im}[T_{\eta f}(f)] = 2\pi f \rho \frac{\pi D^2}{4} \sqrt{\frac{g}{d}} C_{mf}(f) \quad (29)$$

From linear wave theory the Fourier transformation of kinematics can be related to surface elevation by:

$$U(f) = T_{\eta u}(f) \int_{-\infty}^{\infty} \eta(t) e^{-i2\pi f t} dt = T_{\eta u}(f) H(f) \quad (30)$$

where  $H(f)$  is the Fourier transform of the surface elevation.

Using the asymptotic value of the cosh function, the velocity transfer function  $q$  given by Equation 23 simplifies to a constant and can be written as  $q \approx \sqrt{\frac{g}{d}}$ . This assumption can be made

when the analysis is limited to long waves. By using this expression for transfer function then the hydrodynamic coefficients can be determined from Equations 29 without using wave-by-wave methods.

This model can be extended for the non-linear form of Morison's equation where a cubic approximation is used.

**3.3 Frequency Domain Analysis Using Least Squares** In the frequency domain the hydrodynamics force coefficients can be determined from the spectral density of force using the least square

method.

Using linearization of the drag term in Morison's equation and ensemble averaging with the Gaussian random wave model, Borgman [18] showed that the corresponding power spectral density for  $f(t)$  is:

$$S_f(f) = \frac{8K_D^2 \sigma_u^2}{\pi} S_u(f) + K_M^2 S_{\dot{u}}(f) \quad (31)$$

where  $S()$  denotes the power spectral density of a record (force, velocity and acceleration respectively).

When there is a current in addition to waves then Equation 31 may be shown (Li & Kang, 1992) to take the form:

$$S_f(f) = 16(z(\gamma) + |\gamma| Z(\gamma))^2 K_D^2 \sigma_u^2 S_u(f) + K_M^2 S_{\dot{u}}(f) \quad (32)$$

where the terms have the same meaning as in Equation 3.

Using linear wave theory the spectral densities of velocity and acceleration are related to the spectral density of the sea surface  $S_\eta(f)$ , by:

$$S_u(f) = \left( \frac{(2\pi f)^2 \cosh^2 kz}{\sinh^2 kd} \right) S_\eta(f) \quad (33)$$

$$S_{\dot{u}}(f) = (2\pi f)^2 S_u(f)$$

Using the least squares method in the form corresponding to that given in [19],  $K_M$  and  $K_D$  is given by:

$$K_M^2 = \frac{\sum_{i=1}^N S_u(\omega_i) S_{\dot{u}}(\omega_i) \sum_{i=1}^N S_u(\omega_i) S_f(\omega_i)}{M} \quad (34)$$

$$- \frac{\sum_{i=1}^N S_u^2(\omega_i) \sum_{i=1}^N S_{\dot{u}}(\omega_i) S_f(\omega_i)}{M}$$

$$K_D^2 = \left( \frac{\sum_{i=1}^N S_u(\omega_i) S_{\dot{u}}(\omega_i) \sum_{i=1}^N S_{\dot{u}}(\omega_i) S_f(\omega_i)}{M} - \frac{\sum_{i=1}^N S_u^2(\omega_i) \sum_{i=1}^N S_u(\omega_i) S_f(\omega_i)}{M} \right) \left( \frac{\pi}{8\sigma_u^2} \right) \quad (35)$$

where

$$M = \left( \sum_{i=1}^N S_u(\omega_i) S_{\dot{u}}(\omega_i) \right)^2 - \sum_{i=1}^N S_u^2(\omega_i) \sum_{i=1}^N S_{\dot{u}}^2(\omega_i)$$

where  $N$  is the number of discrete frequencies at which the spectrum is computed from the time series analysis and all the spectral densities are determined from the time histories. In laboratory experiments where the velocity time history is available the first part of Equation 33 does not need to be used.

It should be noted that the accuracy of this method for evaluating  $C_M$  and  $C_D$  may be limited due to the first order linear approximation of velocity on the one hand and the possible unsuitability of the data for the least square method according to Dean's reliability ratio on the other hand.

**3.4 Cross-Spectral Density Fitting** The hydrodynamic force coefficients can be obtained from the cross-spectral density between surface elevation and wave force as indicated in [20]. Using this method and considering a linearization of the Morison's equation the cross-spectrum of waves and wave force can be obtained as follows

$$S_{\eta f}(f) = \sqrt{\frac{8}{\pi}} K_D \sigma_u S_{\eta u}(f) + K_M S_{\eta \dot{u}}(f) \quad (36)$$

where  $S_{\eta f}(f)$ ,  $S_{\eta u}(f)$  and  $S_{\eta \dot{u}}(f)$  are cross-spectra of wave surface elevation and force, velocity and acceleration respectively. These three cross-spectra may be estimated from measured data and can be divided into the real and imaginary parts, so that the force coefficients as functions of

frequency may be obtained as:

$$C_d(f) = \sqrt{\frac{\pi}{8}} \frac{2}{\rho D \sigma_u} \left( \frac{C_{\eta\dot{u}} Q_{\eta f} - Q_{\eta\dot{u}} C_{\eta f}}{C_{\eta\dot{u}} Q_{\eta u} - Q_{\eta\dot{u}} C_{\eta u}} \right) \quad (37)$$

$$C_m(f) = \frac{4}{\rho \pi D^2} \left( \frac{C_{\eta f} Q_{\eta u} - C_{\eta u} Q_{\eta f}}{C_{\eta\dot{u}} Q_{\eta u} - Q_{\eta\dot{u}} C_{\eta u}} \right) \quad (38)$$

where  $C_{ij}$  and  $Q_{ij}$  indicate the real and imaginary part of cross-spectra of the two time series (I & j) and the subscribes of  $\eta$ ,  $u$ ,  $\dot{u}$  and  $f$  indicate to surface elevation, velocity, acceleration and force time series respectively.

In the case of current as well as waves then Equation 36 may be written as:

$$S_{\eta f}(f) = 4(z(\gamma) + |\gamma| Z(\gamma)) K_D \sigma_u S_{\eta u}(f) + K_M S_{\eta \dot{u}}(f) \quad (39)$$

and the drag coefficient is given by:

$$C_d(f) = \frac{1}{2\rho D \sigma_u (z(\gamma) + |\gamma| Z(\gamma))} \times \left( \frac{C_{\eta\dot{u}} Q_{\eta f} - Q_{\eta\dot{u}} C_{\eta f}}{C_{\eta\dot{u}} Q_{\eta u} - Q_{\eta\dot{u}} C_{\eta u}} \right) \quad (40)$$

The inertia coefficient remains the same as Equation 38.

The frequency-dependent parameters of  $C_d(f)$  and  $C_m(f)$ , may only have validity in the range of frequencies where most of the wave energy (about 90 %) is concentrated. A fuller discussion of these methods, their approximations and practical limitations is given in [6].

#### 4. ESTIMATING WAVE PARTICLE KINEMATICS FROM WAVE SURFACE MEASUREMENTS

The computation of water particle kinematics is one of the most important tasks in the determination of force on slender offshore structures where

Morison's equation is used.

It is shown through this paper that the uncertainties in the estimation of kinematics can play an important role in comparing with uncertainties of hydrodynamic coefficients ( $C_d$  and  $C_m$ ). These uncertainties are relative to using different methodology of  $C_d$  and  $C_m$  and different wave kinematics models. A comparison in this paper shows that the choice of wave theory represents a choice with a large impact on the corresponding force.

The simplest approach to the prediction of kinematics is to use linear theory. This method cannot give good accuracy at the near surface due to the non-linearity of the free surface boundary condition.

Stokes' theory is widely used in the design and analysis of offshore structures, and in this paper fifth-order, third-order and first-order (Airy theory or linear theory) Stokes theory are considered. In this study because the current exists in most of the experiments, Fenton's method [21] has been used to predict the wave kinematics from surface elevation. The details of the description and formulation of this method are given by (e.g. [22]) and are not repeated here.

Each random wave in a record has been replaced with a single deterministic wave, and then the corresponding velocity and acceleration time series have been obtained through wave-by-wave analysis using each wave theory in turn. This predicted kinematics has been compared with the measured ones.

In the De Voorst wave flume the beach is not perfect and the coefficient of wave reflection is about 0.1 over most of the range of frequencies used in the experiments described here.

Guza, et al. [23] developed a time domain method to decompose the long waves into seaward and shoreward propagating components by using a pressure gage and current meter located on the same vertical line in the water column. The detail of this method is given in [24] and in this paper that method has used for the decomposition of surface elevation time series into the incident and reflected wave train. It can be shown that the incident and reflected wave train ( $\eta_i$  and  $\eta_r$ ) are given by



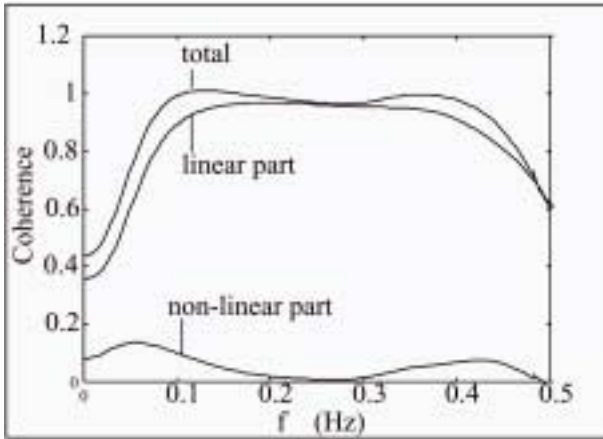


**Figure 1.** Coherence Function for Run 1 (Using System Identification Technique, Non-Linear Model).

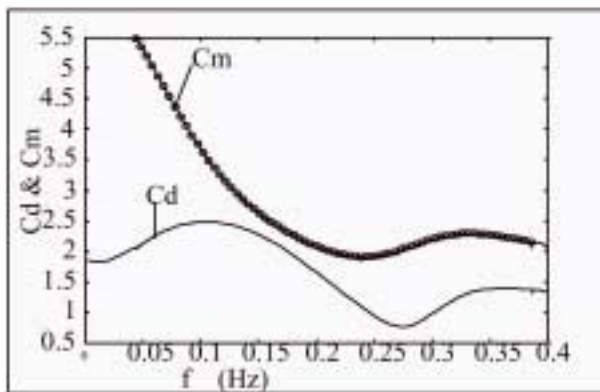


**Figure 2.** Variation of  $C_d$  and  $C_m$  with Frequency Using System Identification Technique, Non-Linear Model, (Run1).

$$\begin{aligned} \eta_r(t) &= \frac{1}{2}[\eta(t) - u(t)\sqrt{\frac{d}{g}}] \\ \eta_i(t) &= \frac{1}{2}[\eta(t) + u(t)\sqrt{\frac{d}{g}}] \end{aligned} \quad (41)$$

By using the Airy theory, Stokes' third and fifth order theory (Fenton method) and using the incident and reflected wave time series the corresponding horizontal wave particle kinematics are estimated.

## 5. DISCUSSION OF RESULTS

### 5.1 Variation of Force Coefficients and Predictive Accuracy with Analysis Method

Tables 1, 2 show the mean values of  $C_d$  and  $C_m$  obtained using the various analysis methods described in Section 3.

The system identification approach is only considered here for the cases where there is no current. The author obtained very poor results when attempts were made to include current and these results are not included. The addition of the non-linear term makes little difference for the large pile case, as could be predicted from examination of the coherence function shown in Figure 1. Interestingly the non-linear term does make a contribution to the coherence function at the high frequency and for the small pile, Figure 3, but the overall result is a very distinct decrease in predictive accuracy both in terms of RMSE and bias.

Consider now the results obtained using frequency domain spectral analysis methods, which assume linear wave theory and have been applied to the entire time series of each run rather than on a wave-by-wave basis. The least squares (or "auto-spectral") method gives single values of  $C_d$  and  $C_m$  irrespective of frequency as can be seen from Equations 34 and 35.

The "cross spectral" method produces  $C_d$  and  $C_m$  values which are functions of frequency as can be seen from Equations 37 and 38 and in Figures 5 and 6 which shows the results obtained for fixed large pile and mobile small pile respectively. The standard deviations quoted in Tables 1-3 relate to this variation with frequency. The cross-spectral method consistently gives lower values of  $C_d$  than the "auto-spectral" method and generally has higher predictive accuracy.

### 5.2 Predicting Particle Kinematics from Wave Surface Elevation

It is just wave height and period that are available to represent offshore wave conditions in the majority of cases. The prediction of wave particle kinematics from the wave height and period measured during the experiments using various wave theories has been compared with the measured particle velocities. The results are presented in Table 4 for the case

**TABLE 1. Values of  $C_m$  and  $C_d$  from the Analysis Methods in the Random Waves for a Fixed Large Pile (Run 1).**

Methods of Analysis		$C_d(\text{mean})$	$\sigma_{C_d}$	$C_m(\text{mean})$	$\sigma_{C_m}$	%MNE	%rmse
System Identification Method	Linear	1.41	0.40	1.93	0.44	11.03	14.70
	non-linear	1.42	0.58	1.93	0.44	10.93	14.63
	surf. elev. $C_r^*=0$	1.66	0.28	1.96	0.81	7.56	12.67
	surf. elev. $C_r^*=0.05$	2.02	0.34	2.17	0.90	-4.16	12.69
Spectral Analysis	auto-spectrum	2.26	---	1.87	---	1.94	14.54
	cross-spectrum	1.57	0.69	1.95	1.08	8.70	13.24
mean value		1.72	0.46	1.97	0.73	6.00	13.75

**TABLE 2. Values of  $C_m$  and  $C_d$  from the Analysis Methods in the Random Waves for a Mobile Large Pile (Run 2).**

Methods of Analysis		$C_d(\text{mean})$	$\sigma_{C_d}$	$C_m(\text{mean})$	$\sigma_{C_m}$	%MNE	rmse%
Spectral Analysis	auto-spectrum	1.14	---	2.32	---	22.6	23.4
	cross-spectrum	1.10	0.49	2.34	1.31	24.81	25.55
Mean value		1.12	0.49	2.33	1.31	23.70	24.47

**TABLE 3. Values of  $C_m$  and  $C_d$  from the Analysis Methods in the Random Waves (Averaged in the Six Runs).**

Methods of Analysis		% bias	% RMSE	$C_d(\text{mean})$	$C_m(\text{mean})$
Frequency Domain (System Identification Method)	linear	8.35	15.83	1.58	1.82
	non-linear	16.43	19.68	1.35	1.89
	surf. elev. $C_r^*=0$	14.42	18.55	1.52	1.81
	surf. elev. $C_r^*=0.05$	5.32	14.49	1.86	2.00
Spectral Analysis	auto-spectrum	24.14	30.80	1.82	1.79
	cross-spectrum	15.93	20.6	1.47	1.98
mean value		14.10	19.99	1.60	1.88

**TABLE 4. Accuracy of Prediction of Water Particle Velocity and Acceleration in the Random Waves with Different Current Speeds (Reflection was Considered).**

Data	Wave theory	velocity error		acceleration error	
		MNE%	%RMSE	MNE%	RMSE%
Run1	linear	7.90	17.50	6.23	17.18
	Stokes 3rd	8.07	18.35	9.43	18.24
	Stokes 5th	8.53	18.45	9.67	18.21
Run2	linear	1.30	8.11	11.39	20.76
	Stokes 3rd	-0.70	8.40	12.03	20.57
	Stokes 5th	-0.45	8.36	12.57	20.82
%Mean error (for 6Runs)	linear	5.67	13.25	12.35	21.26
	Stokes 3rd	6.60	14.96	14.22	21.87
	Stokes 5th	6.73	14.81	14.75	22.24

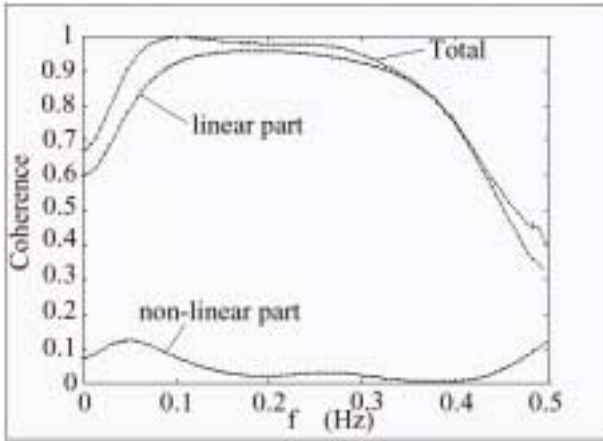


**Figure 3.** Coherence function for Run 4 (using system identification technique, non-linear model).

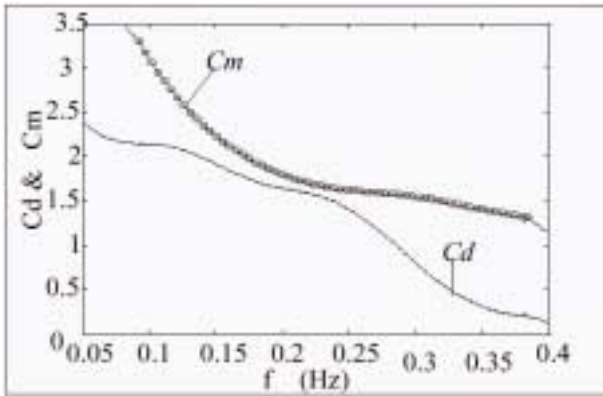


**Figure 4.** Variation of  $C_d$  and  $C_m$  with frequency using system identification technique, non-linear model, (Run 4).

where reflection is considered using the linear approach discussed in Section 4. The reflection coefficient is around 0.1 for the range of frequencies over which at least 90% of the wave energy is concentrated. In these Tables the reference acceleration has been obtained by differentiating the smoothed measured velocity signal.

When no correction for reflection is made the velocity predicted from the wave height and period is in all cases (except Run6) larger than the measured velocity. Interestingly both the average bias and the RMSE are least, by a small margin, for linear wave theory. When a correction for reflection is made the particle velocities are underestimated with bias of around 6% and the

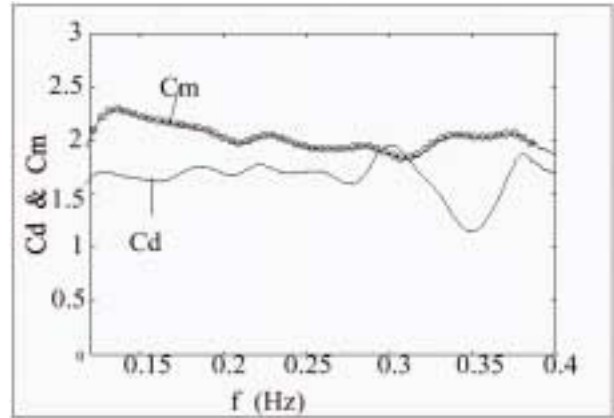


**Figure 5.** Variation of  $C_d$  and  $C_m$  with often frequencies using cross-spectral density fitting (fixed large pile Run1)

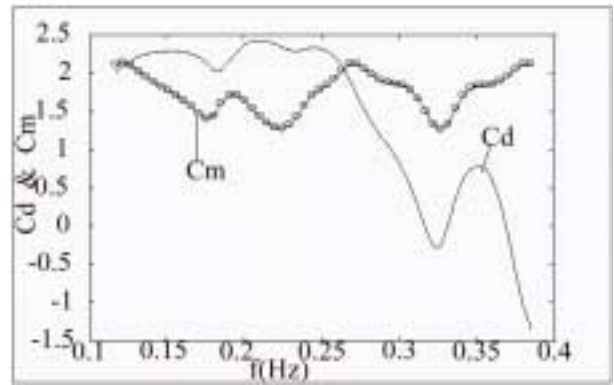


**Figure 6.** Variation of  $C_d$  &  $C_m$  with often frequencies using cross-spectral density fitting (mobile small pile,  $U=-0.5$  m/sec Run6).

RMSE for the velocities are lower. Interestingly linear theory appears to give the best results whether or not reflection is considered. This might in part be attributed to the fact that the correction for reflection is based on linear theory. What the results illustrate is the difficulty in predicting wave particle kinematics from surface elevation even when there is just a relatively small amount of wave reflection in a wave flume. In real sea conditions, where the wave energy may be spread all a wide range of directions, prediction of particle kinematics will probably result in errors of at least these magnitudes. This highlights the value of direct measurement of water particle kinematics in the wavetank (and offshore).

## 6. CONCLUSIONS

It is clear that the method used to analyze experiment data in terms of Morison's equation has a significant affect on both the force coefficients obtained and their predictive accuracy. It is found that no single method is consistently better under all circumstances. The other analysis methods whilst a little poorer worked satisfactorily except for the auto- and cross-spectral analysis approaches which gave some extreme results are susceptible to numerical instability and should be avoided.

When particle kinematics are not available and have to be inferred from surface elevation the errors increase. The additional error associated with particle kinematics prediction is not significantly reduced when account is taken of reflected waves using linear correction. Linear wave theory was significantly better than Stokes' third order and marginally better than fifth order theory at predicting particle kinematics. The average bias and RMSE in predicted force, for all methods and all experiment runs, were -8% and 29% respectively, indicating that if at all possible water particle kinematics should be measured directly. If this is not possible then using a Systems Identification approach as outlined in Section 3.2 seems to give the best result as can be seen from the bias and RMSE given in Table 3.

## 7. REFERENCES

1. Sarpkaya, T. and Isaacson, M., "Mechanics of Forces on Offshore Structures", Van Nostrand Reinhold Company Inc., New York, (1981).
2. Rodenbusch, G. and Gutierrez, C. A., "Forces on Cylinders in Two-Dimensional Flows", *Technical Progress Report*, BRC 13-83, Shell Development Co., (1983).
3. Bearman, P. W., Chaplin, J. R., Graham, J. M. R., Kostense, J. K., Hall, P. F. and Klopman, G., "The Loading on a Cylinder in Post-Critical Flow Beneath Periodic and Random Waves", *Behavior of Offshore Structures*, (1985), 213-225.
4. Bishop, J. R., "Wave Force Investigation at the Second Christchurch Bay Tower", *Summary Report, NMI R177*, OT-O-82100, (1984).
5. Wolfram, J. and Naghipour, M., "On the Estimation of Morison Force Coefficients and Their Predictive Accuracy for Very Rough Circular Cylinders", *Applied Ocean Research*, Vol. 21, (1999), 311-328.
6. Naghipour, M., "The Accuracy of Hydrodynamic Force Prediction for Offshore Structures and Morison's Equation", Thesis submitted for Ph.D., Heriot-Watt University, Edinburgh, (1996).
7. Chen, S. and Billings, S. A., "Modeling and Analysis of Non-Linear Time Series", *Int. J. Control*, Vol. 50, No. 6, (1989), 2151-2171.
8. Kaplan, P., Jiang, C. W. R. and Stritto, F. J. D., "Determination of Offshore Structure Morison's Equation Force Coefficients Via System Identification Techniques", *International Symposium on Hydrodynamics in Ocean Engineering*, The Norwegian institute of Technology, (1981), 469-489.
9. Bendat, J. S. and Piersol, A. G., "Decomposition of Wave Forces into Linear and Non-Linear Components", *Journal of Sound and Vibration*, Vol. 106, No. 3, (1986), 391-408.
10. Vugts, J. H. and Bouquet, A. G., "A Non-Linear, Frequency Domain Description of Wave Forces on an Element of a Vertical Pile in Random Seas Behavior of offshore Structures", Elsevier Science Publishers B.V., Amsterdam, 1985-Printed in the Netherlands, (1985), 239-253.
11. Blik, A. and Klopman, G., "Non-Linear Frequency Modeling of Wave Forces on Large Vertical and Horizontal Cylinders in Random Waves", *BOSS' 88*, (1988), 821-840.
12. Borgman, L. E., "Ocean Wave Simulation for Engineering Design", *J. of the Waterways and Harbours Div., Proc. of the ASCE*, Vol. 95, No. WW4, (1969), 557-583.
13. Bendat, J. S. and Piersol, A. G., "Random Data, Analysis and Measurement Procedures", Second Edition, John Wiley & Sons, New York, (1986).
14. Newland, D. E., "An Introduction to Random Vibrations and Spectral Analysis", Third Edition, Longman Inc., New York, (1993).
15. Schetzen, M., "The Volterra and Wiener Theories of Non-Linear Systems", John Wiley and Sons, New York, (1980).
16. Worden, K., Stansby, P. K., Tomlinson, G. R. and Billings, S. A., "Identification of Non-Linear Wave Forces", *Journal of Fluids and Structures*, No. 8, (1994), 19-71.
17. Li, Y. C. and Kang, H. G., "Wave Current Forces on Slender Circular Cylinder", *Proc. of the 11th Int. Conf. on Offshore Mechanics and Arctic Engineering (OMAE)*, Vol. 1-A, (1992), 117-125.
18. Borgman, L. E., "Spectral Analysis of Ocean Wave Forces on Piling", *J. of the Waterways and Harbours Div., Proc. of the ASCE*, Vol. 93, No. WW2, (1967), 129-156.
19. Naghipour, M., "Large Scale Experiments Data Analysis for Estimation of Hydrodynamic Force Coefficients Part1: Time Domain Analysis", *International Journal of Engineering*, Vol. 14, No. 4, (2001), 323-332.
20. Borgman, L. E., "Statistical Models for Ocean Waves and Wave Forces", *Advanced in Hydroscience*, Vol. 8, (1972), 139-181.
21. Fenton, J. D., "A Fifth-Order Stokes Theory for Steady Waves", *Journal of Waterway, Port, Coastal, and Ocean Engineering*, Vol. 111, No. 2, (1985), 216-234.
22. Sobey, R. J., Goodwin, P., Thieke, R. J. and Westberg, Jr., "Application of Stokes, Cnoidal, and Fourier Wave Theories", *Journal of Waterway, Port, Coastal, and Ocean Engineering*, Vol. 113, No. 6, (1987), 565-587.
23. Guza, R. T., Thornton, E. B. and Holman, R. A., "Swash on Steep and Shallow Beaches", *Proc. of the 19th Coastal Engineering Conference, ASCE*, Vol. 1, (1984), 708-723.
24. Hughes, S. A., "Physical Models and Laboratory Techniques in Coastal Engineering", World Scientific, London, (1993).